

Cavity ringdown spectroscopy measurements of the infrared water vapor continuum

John G. Cornier, Roman Ciurylo, and James R. Drummond

Citation: *The Journal of Chemical Physics* **116**, 1030 (2002); doi: 10.1063/1.1425825

View online: <http://dx.doi.org/10.1063/1.1425825>

View Table of Contents: <http://scitation.aip.org/content/aip/journal/jcp/116/3?ver=pdfcov>

Published by the [AIP Publishing](#)

Articles you may be interested in

[Absolute molecular transition frequencies measured by three cavity-enhanced spectroscopy techniques](#)

J. Chem. Phys. **144**, 214202 (2016); 10.1063/1.4952651

[On the Application of Cavity Ringdown Spectroscopy to Measurements of Line Shapes and Continuum Absorption](#)

AIP Conf. Proc. **645**, 401 (2002); 10.1063/1.1525481

[Single-mode cavity ring-down spectroscopy for line shape measurements](#)

AIP Conf. Proc. **467**, 275 (1999); 10.1063/1.58318

[Cavity-locked ring-down spectroscopy](#)

J. Appl. Phys. **83**, 3991 (1998); 10.1063/1.367155

[Laser diode cavity ring-down spectroscopy using acousto-optic modulator stabilization](#)

J. Appl. Phys. **82**, 3199 (1997); 10.1063/1.365688



NEW Special Topic Sections

NOW ONLINE
Lithium Niobate Properties and Applications:
Reviews of Emerging Trends

AIP | Applied Physics
Reviews

Cavity ringdown spectroscopy measurements of the infrared water vapor continuum

John G. Cormier,^{a)} Roman Ciurylo,^{b)} and James R. Drummond

Department of Physics, University of Toronto, 60 St. George Street, Toronto, Ontario, M5S 1A7 Canada

(Received 11 July 2001; accepted 15 October 2001)

We report measurements of the water vapor continuum using infrared cavity ringdown spectroscopy at frequencies of 931.002, 944.195, and 969.104 cm^{-1} . Our values of the water vapor continuum coefficients for self-broadening at $T=296\text{ K}$ are $C_s^0(931\text{ cm}^{-1})=2.23\pm 0.17$, $C_s^0(944\text{ cm}^{-1})=2.02\pm 0.13$, and $C_s^0(969\text{ cm}^{-1})=1.79\pm 0.21\times 10^{-22}\text{ molecules}^{-1}\text{ cm}^2\text{ atm}^{-1}$. Our measurements are found to be in good agreement with the far wing line shape theory of Ma and Tipping, but we find that empirical models of the water vapor continuum, widely used in radiative transfer calculations, significantly overestimate the observed self-broadened continuum. © 2002 American Institute of Physics. [DOI: 10.1063/1.1425825]

I. INTRODUCTION

The infrared absorption due to water vapor is a long-standing experimental and theoretical problem.^{1–7} The absorption coefficient of water vapor is the sum of contributions from local lines and a weak, unstructured background known as the water vapor continuum,

$$k(\nu) = k_l(\nu) + k_c(\nu), \quad (1)$$

where k_l and k_c are the local line and continuum absorption coefficients (cm^{-1}), respectively. Local line absorption is defined as being a Lorentz profile at these pressures, truncated $\pm 25\text{ cm}^{-1}$ from line center. Thus, the continuum is the remaining water vapor absorption which is not considered local line absorption.

The water vapor continuum is described in terms of the following empirical relation:^{8,9}

$$k_c(\nu, T) = \left(\frac{N_0}{P_{\text{ref}}} \right) \left(\frac{T_{\text{ref}}}{T} \right) [C_s(\nu, T) \times e^2 + C_f(\nu, T) \times e P_f], \quad (2)$$

where P_{ref} is the reference pressure (1 atm), T_{ref} is the reference temperature (296 K), N_0 is the number density of an ideal gas at the reference conditions (molecules cm^{-3}), e is the water vapor partial pressure (atm), P_f is the foreign gas partial pressure (atm), and C_s and C_f are known as the continuum coefficients for self- and foreign-broadening, respectively ($\text{molecules}^{-1}\text{ cm}^2\text{ atm}^{-1}$). Notably, the continuum has a strong quadratic dependence on the water vapor partial pressure.

The water vapor continuum spans the infrared spectrum,¹⁰ but it is more difficult to measure in the presence of strong absorption lines, and so most observations have been made in the relatively transparent thermal infrared window from $\nu=700$ to 1250 cm^{-1} . Even here, measurements

of the continuum present a formidable experimental challenge because the continuous spectrum is smooth and slowly varying, and therefore lacks a clear spectroscopic “signature.” These properties are similar in character to the experimental baseline that one usually seeks to remove from absorption spectra, and so experiments must have a well-characterized baseline in order to make accurate measurements of the continuum. The room-temperature continuum absorption coefficient k_c is of order 10^{-6} cm^{-1} near $\nu=1000\text{ cm}^{-1}$, which is too weak to directly observe over short path lengths at room temperature. Thus, it is necessary to employ techniques which are sensitive to weak absorption, such as conventional multipass cells (e.g., white cells)^{9,11} and photoacoustic spectroscopy.^{12–14}

Several published values of the water vapor continuum coefficient for self-broadening were compared by Hinderling,¹⁴ and these were found to have a scatter of $\pm 35\%$. Grant presented a more extensive comparison of field and laboratory observations,¹⁵ from which the uncertainty in C_s (for a given temperature and wavenumber) is estimated to be $\pm 20\%$. In this paper we determine water vapor continuum coefficients of self-broadening using cavity ringdown spectroscopy. Our results demonstrate that the empirical models of the water vapor continuum which are commonly used in atmospheric radiative transfer calculations^{10,16} overestimate the continuum absorption by 10%–15%. We also note that a far wing line shape theory has recently been developed,^{17,18} and continuum absorption coefficients derived from this theory are found to be in good agreement with our observations.

II. CAVITY RINGDOWN SPECTROSCOPY

Introduced in 1988,¹⁹ cavity ringdown spectroscopy (CRDS) has developed into a powerful technique for the quantitative measurement of weak gas absorption.^{20–26} In CRDS, a laser pulse is injected into a high-finesse, stable optical cavity (the “ringdown cavity”) via the transmission loss of the front mirror, and the time evolution of the energy circulating inside the ringdown cavity is observed through

^{a)}Author to whom correspondence should be addressed. Electronic mail: cormier@atmosph.physics.utoronto.ca

^{b)}Permanent address: Institute of Physics, Nicholas Copernicus University, Grudziadzka 5/7 87-100 Toruń, Poland.

the transmission loss of the back mirror. For an unsaturated medium, monochromatic energy trapped inside the cavity will obey the relation,

$$I(t) = I_0 \exp(-t/\tau), \quad (3)$$

where τ is the decay time constant.

Although independently developed, the principles behind our CRDS experiment are similar to those of the pulsed, single-mode CRDS near-infrared experiment of van Zee *et al.*^{25,26} In single-mode CRDS, the decay time constant may be expressed as

$$\tau(\nu) = \frac{L}{c[(1-R) + k_{bg}(\nu)L + k(\nu)L]}, \quad (4)$$

where L is the ringdown cavity mirror separation, c is the speed of light, and R is the effective reflectivity of the mirrors. The term $(1-R)$ refers to the intrinsic cavity loss per pass. The presence of a gaseous medium in the ringdown cavity requires the addition of two other loss factors: $k(\nu)$ is the absorption of the gas (cm^{-1}), while $k_{bg}(\nu)$ represents any other loss mechanism associated with the medium (e.g., Rayleigh scattering or trace gas contamination).

Because of the continuous nature of the water vapor continuum absorption, it is not possible to detune the experiment from an absorption peak in order to obtain the empty-cell decay constant [i.e., $k_c(\nu) \neq 0$, for any ν]. Therefore, we have developed a flow experiment where we control the amount of water vapor in the flow from zero to near saturation. Since the water vapor accounts for a small fraction of the total gas pressure (0–2%, at room temperature), we make the assumption that any background loss associated with the medium is taken into account in the dry nitrogen flow. In other words, the dry flow decay constant τ_0 is given by

$$\tau_0(\nu) = \frac{L}{c[(1-R) + k_{bg}(\nu)L]}. \quad (5)$$

From consideration of Eqs. (4) and (5), we may obtain the following simple expression for the absorption coefficient:

$$k(\nu) = \frac{\tau_0(\nu) - \tau(\nu)}{c\tau_0(\nu)\tau(\nu)}. \quad (6)$$

It is apparent from Eq. (6) that the absorption coefficient k is directly determined from measurements of the decay constant alone, and in particular does not require knowledge of either the ringdown cavity length or the mirror reflectivity.

For our application, CRDS has distinct advantages over conventional spectroscopic techniques. In particular, CRDS provides a direct measure of the absorption coefficient in terms of observed ringdown times, and can be realized with high sensitivity using relatively small sample volumes, which facilitates gas handling and control. For example, our ringdown cavity has a gas volume of 6 liters and an effective path length of 720 m. The impressive sensitivity of CRDS is achieved through accurate measurements of the energy decay rate in the cavity (rather than measurements of transmission), and so CRDS is independent of laser intensity fluctuations. While much important CRDS work has occurred in the visible and near-infrared regions where high reflectivity mirrors

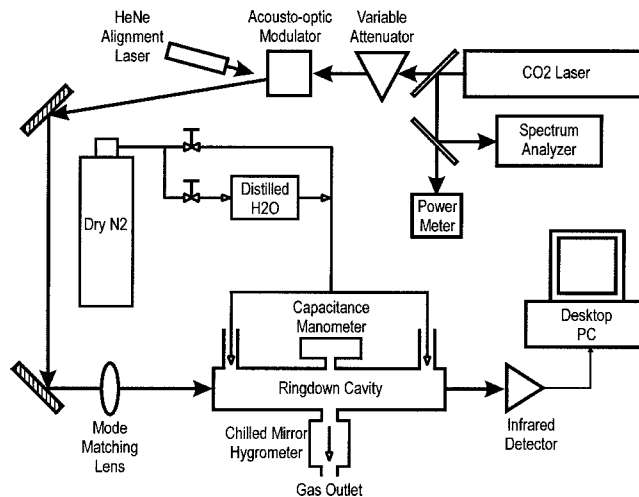


FIG. 1. Schematic of the infrared cavity ringdown spectroscopy experiment. The main optical beam moves anticlockwise through the apparatus from the CO_2 laser at top right, to the detector at bottom right.

are available, we demonstrate that high sensitivity is also possible in the thermal infrared region of the spectrum with mirrors of modest reflectivity.

III. EXPERIMENT

The layout of our experiment is illustrated in Fig. 1. The source of infrared radiation is a line-tunable cw CO_2 laser. A beamsplitter directs a portion of the beam to a power meter and a calibrated diffraction grating spectrum analyzer to identify the CO_2 laser transition. The laser is normally operated on the $10P(20)$ transition, $\nu = 944.195 \text{ cm}^{-1}$, and has an output power of $\sim 6 \text{ W}$ and a bandwidth $\leq 250 \text{ kHz}$. In the CRDS experiment, pulses shaped from the first-order deflected beam from an acousto-optic modulator (AOM) are mode-matched and coupled into the ringdown cavity. The laser beam is attenuated with a polarizer-analyzer-attenuator stack of Brewster plates so that $\sim 1 \text{ mW}$ of power is incident on the ringdown cavity. All of the measurements we report herein were obtained using $5 \mu\text{s}$ long laser pulses at a repetition rate of 2500 Hz .

The gas for the experiment is obtained from commercial cylinders of nitrogen with a rated purity of 99.998%. The flow from the cylinders is split into two paths and needle valves are used to control the fraction of the flow which passes over a body of distilled water before the flow paths are recombined. Inside the ringdown gas cell, the pressure and temperature are measured with a capacitance manometer and a thermocouple sensor, respectively. The flow dewpoint is measured at the exhaust port of the ringdown gas cell using a chilled mirror hygrometer (EdgeTech Model 200 Dewtrak) which has been NIST-calibrated. The dewpoint is converted to a water vapor partial pressure using the formulas of Wexler.^{27,28} The accuracy of the measured dewpoint is $\pm 0.2 \text{ K}$, which corresponds to a water vapor partial pressure uncertainty ranging from $\pm 1.9\%$ for the lowest humidities considered, to $\pm 1.3\%$ for the highest humidities.

The ringdown cavity is formed by two 100 cm radius of curvature spaced a distance of 102.5 cm apart. The cavity

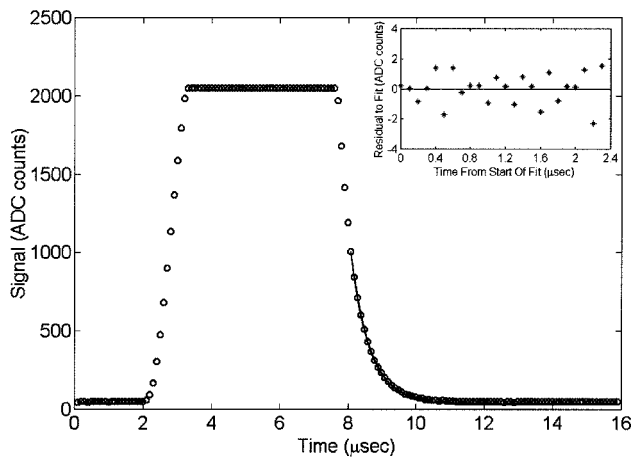


FIG. 2. Typical ringdown event as a function of time. The first 2 μs are background. During the period from ~ 3 to 8 μs the detector electronics saturate as laser energy is being injected into the ringdown cavity. This is followed by the “ringdown” decay event. The best fit to the data is shown as a solid line in the interval 8.1–10.4 μs . The residuals to the fit can be seen in the inlay (note expanded scale).

length is stabilized by three Zerodur(tm) zero-thermal-expansion ceramic glass rods. The 2.54 cm diam mirrors consist of dielectric coatings layered on ZnSe substrates, and were manufactured to have a reflectivity $R=0.994$ at $\nu=944\text{ cm}^{-1}$. Our near-confocal ringdown cavity therefore has a free spectral range of about 150 MHz, and a finesse of about 600. One of the mirrors is mounted on a piezoelectric transducer (PZT) so that the resonant frequency of the ringdown cavity may be fine-tuned. The alignment of optics is performed with the assistance of a HeNe laser which is adjusted to be coaxial with the infrared laser pulses. Infrared radiation enters and exits the gas cell via (antireflection-coated) ZnSe windows on the end flanges.

The mode-matching optics ensures that only the TEM_{00} and TEM_{01} modes can be excited in the ringdown cavity. However, the TEM_{01} mode does not cause a problem in our experiment because it is separated from the TEM_{00} mode by 70 MHz and our optical excitation bandwidth is about 0.25 MHz. We obtain pure excitation of the TEM_{00} mode by tuning the PZT to the transmission peak of that mode.

The energy decay inside the ringdown cavity is observed with a liquid-nitrogen cooled HgCdTe photovoltaic detector (50 MHz electrical bandwidth) at the output end of the gas cell. The signal from the dc-coupled output of the detector is sampled by a 12-bit analog-to-digital converter (Datel Model PCI-416H) at a rate of 10 Msamples/s.

IV. DATA ANALYSIS AND RESULTS

The data are analyzed on a shot-by-shot basis. A typical ringdown event is shown in Fig. 2. The initial portion of the event is a 2 μs long pretrigger sample from which we estimate the baseline signal of the infrared detector. Following this, the AOM is triggered and the signal rises rapidly as the laser pulse is injected into the ringdown cavity. The digitized signal appears flat during the period between 3.3–7.6 μs because the detector output exceeds the +5 V digitization

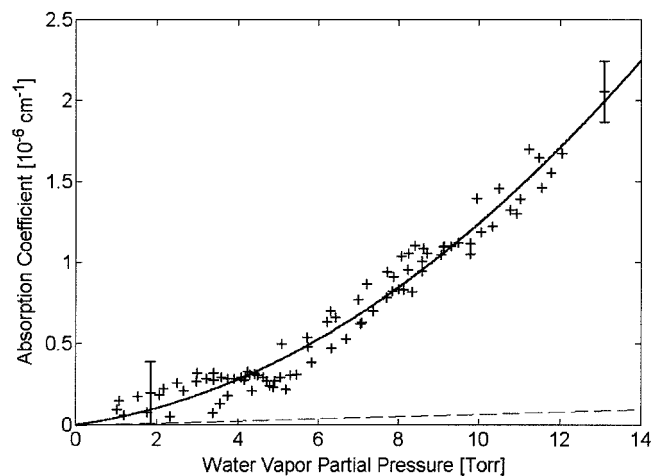


FIG. 3. Water vapor continuum absorption coefficients for 944 cm^{-1} and 294 K. The “+” are the continuum absorption coefficients k_c , while the dashed line is the local line absorption coefficient k_l . The solid line is the least squares fit of the measured continuum absorption coefficients to Eq. (2). $1-\sigma$ experimental error bars are shown for low and high humidities.

limit of the ADC. This is done to maximize the signal to noise ratio over the decay portion of the ringdown event. It is necessary to wait another 0.5 μs before the AOM shutter has fully closed and the signal is pure exponential decay. The Levenberg—Marquardt least-squares minimization algorithm is used to fit a fixed portion of each decay curve to Eq. (3). In addition to fitting for the initial amplitude and the decay time constant τ , we also fit for the baseline. For each decay event, the starting point of the fit is fixed at 6.1 μs following the trigger which initiates the formation of an optical pulse. The fitting time window, Δt , used for all decay events is 2.4 μs long. Thus, the effective optical path length of our experiment is $L_{\text{eff}} \sim c\Delta t \sim 720\text{ m}$. The residual to the fit is shown in the inlay to Fig. 2. Our residuals are found to be normally distributed, with no evidence of systematic effects. Each absorption coefficient is determined from 2000 individual decay events.

The dry-cell decay constant is $\tau_0 = 546.6 \pm 1.3\text{ ns}$ for $\nu = 944\text{ cm}^{-1}$, which corresponds to an effective mirror reflectivity $R_{\text{eff}} \sim 0.994$. We note the fractional time constant noise, $\sigma_\tau/\tau = 0.2\%$, is much less than the observed shot-to-shot amplitude fluctuations of 2%. This demonstrates, as expected, that CRDS measurements are insensitive to fluctuations in laser intensity, unlike techniques based on transmission measurements.

In the present investigation, we have chosen CO_2 laser lines where the water vapor local line absorption is very small. Nevertheless, local line absorption within $\pm 25\text{ cm}^{-1}$ of the measurement was determined from line-by-line calculations using the HITRAN 2000 molecular database and subtracted from all measured absorption coefficients. At each wave number (laser line), we have made several measurements for different values of the water vapor partial pressure. For example, our measurements of the water vapor continuum absorption coefficients for $\nu = 944\text{ cm}^{-1}$ are presented in Fig. 3. From these data we determine the water vapor continuum coefficients of self- and nitrogen-broadening by a least squares fit to Eq. (2). The continuum

TABLE I. Summary of water vapor continuum measurements. The uncertainty in the continuum coefficients represents the standard deviation to the fit.

CO ₂ laser transition	ν (cm ⁻¹)	Number of measurements	T (K)	Range of water vapor partial pressures (atm)	C_s^0 (10 ⁻²² molecules ⁻¹ cm ² atm ⁻¹)
10P(34)	931.002	39	297.4	0.0038–0.022	2.23±0.17
10P(20)	944.195	88	294.1	0.0017–0.017	2.02±0.13
10R(10)	969.104	39	295.1	0.0021–0.019	1.79±0.21

coefficients of self- and nitrogen-broadening are the only free parameters used in the fit.

In order to compare our values with the results of others, it is convenient to correct our measurements to 296 K. For simplicity, we have adopted the temperature dependence model proposed by Roberts,¹⁶

$$C_s(\nu T) = C_s^0(\nu) \exp \left[T_0 \left(\frac{1}{T} - \frac{1}{296} \right) \right], \quad (7)$$

where C_s^0 is the continuum coefficient of self-broadening at 296 K and T_0 is a characteristic temperature which we have taken to be 1900 K after an examination of Hinderling's data.¹⁴ We do not mean to imply that Eq. (7) is the correct model of the temperature dependence of the water vapor continuum, only that it is adequate for small temperature corrections.

A summary of our experimental results is presented in Table I, demonstrating that it is possible to achieve high sensitivity with cavity ringdown spectroscopy in the 1000 cm⁻¹ region with a very small volume cell.

V. DISCUSSION

Discussions of previous measurements of the continuum can be found in the reviews of Grant¹⁵ and Aref'ev.²⁹ It is illustrative to compare our results with those of other investigators who used CO₂ lasers and multipass cells. As can be seen in Table II, the continuum coefficients of self-broadening measured by others are in excellent agreement with our measurement for 296 K and 944.195 cm⁻¹, but our experimental cell volume is $\sim 1000\times$ smaller.

Empirical models of the water vapor continuum are routinely used in radiative transfer calculations because of their computational efficiency compared to line-by-line calculations of far wing absorption. Two such models are in widespread use. One model,¹⁶ hereafter RSB, is mostly derived from the early laboratory spectrometer data of Burch. The more recent CKD model¹⁰ is also based on Burch's data, but

various field observations have been used to refine the model. As we demonstrate in Fig. 4, both models have continuum coefficients of self-broadening which are substantially higher than our measured values. For the RSB and CKD values of C_s^0 to agree with our results in the 900–1000 cm⁻¹ region, they would have to be scaled down by factors of ~ 0.91 and ~ 0.88 , respectively.

Recently, Ma and Tipping have made significant progress in the development of a far wing line shape theory for water vapor.^{17,18} Beginning with the basic formulation of Rosenkranz,^{34,35} but proceeding in a different way, Ma and Tipping have overcome many of the limitations of that far wing theory. Their far wing line shape theory is based on the binary collision and quasistatic approximations, in which a statistical distribution of stationary molecules was assumed. In the quasistatic approximation, collisions can be considered to be of infinite duration. Thus, the quasistatic approximation is in contrast to the impact approximation (which assumes collisions of infinitesimal duration), from which the Lorentz profile is derived. In Fig. 4 we also compare our measurements of the continuum coefficients of self-broadening to the far wing absorption predicted by Ma and Tipping.¹⁸ The agreement with our results is quite good, which suggests that the far wing theory offers the correct explanation of the water vapor continuum. A significant discrepancy is found for the results at 931 cm⁻¹, which may be evidence of a nearby water dimer combination band. However, the discrepancy might also be attributable to uncertainties in the intermolecular potential which is used in the theoretical calculations. We are currently investigating this possibility and hope to report on progress in a future paper.

VI. CONCLUSION

We have designed a quantitative infrared cavity ringdown spectroscopy experiment capable of making accurate and precise measurements of the water vapor continuum in the $\nu = 900\text{--}1000$ cm⁻¹ region. The experiment uses a

TABLE II. Comparison of water vapor continuum measurements obtained with a CO₂ laser and a multipass cell. Experimental conditions are $T = 296$ K and $\nu = 944.195$ cm⁻¹.

Reference	Method	Cell volume (liters)	C_s^0 (10 ⁻²² molecules ⁻¹ cm ² atm ⁻¹)
Present work	CRDS	6	2.02±0.13
Peterson (1979), Ref. 30	White cell	4400	2.02
Nordstrom (1978), Ref. 31	White cell	4400	2.11
Arefev (1977), Ref. 32	White cell	40000	2.01
McCoy (1969), Ref. 33	White cell	4400	1.94

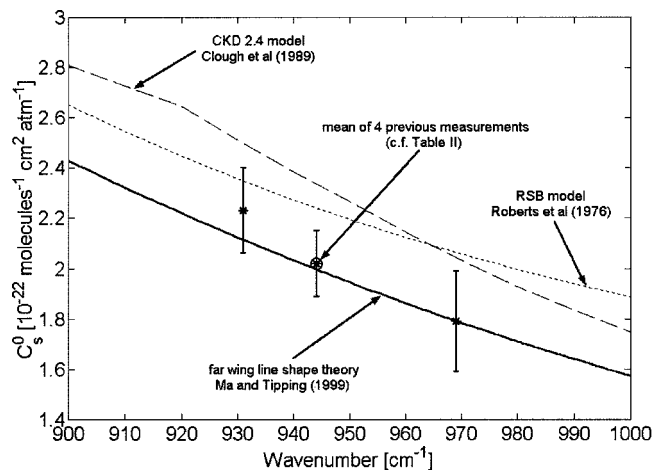


FIG. 4. Comparison of our self-broadened coefficients (*) with the far wing theory of Ma and Tipping (solid line). The mean of four previous measurements (cf. Table II) obtained using CO₂ lasers and multipass cells is shown for 944 cm⁻¹ (circle). Also plotted are the CKD (dashed line) and RSB (dotted line) empirical models of the water vapor continuum.

continuous-wave CO₂ laser and an acousto-optic modulator to create laser pulses which are injected into a 100 cm long near-confocal ringdown cavity. The decay time constants are determined on a shot-by-shot basis, and absorption coefficients are derived from the ensemble statistics of 2000 decay events. Our CRDS experiment is novel, in that it is a gas flow experiment which allows us to control the relative humidity in the flow from zero to near-saturation. Our results demonstrate that this methodology permits us to measure water vapor absorption coefficients with a high degree of accuracy.

Our room temperature measurements of the water vapor continuum are in excellent agreement with the values obtained by other investigators using CO₂ lasers and white cells. The good agreement of our water vapor continuum measurements with the far wing line shape theory of Ma and Tipping suggests that the far wings of water vapor lines are the primary agent responsible for the water vapor continuum. A possible explanation for the discrepancy between our results and the theory of Ma and Tipping near 930 cm⁻¹ may be the presence of a water dimer combination band or uncertainties in the intermolecular potential. We are investigating these possibilities further.

Our results are significantly lower than the values derived from two empirical models of the water vapor continuum. For the RSB and CKD models to agree with our results in the 900–1000 cm⁻¹ region, they would have to be scaled down by factors of ~0.91 and ~0.88, respectively.

Finally, we note there is considerable potential to improve the sensitivity of our experiment, for example with new mirrors or a reduction in time constant noise (e.g., conducting the experiment at a reduced flow rate). This would permit us to investigate other aspects of the water vapor continuum requiring high sensitivity, such as foreign-broadening and low-temperature measurements.

ACKNOWLEDGMENTS

The authors would like to acknowledge the insights and suggestions of J. Patrick Looney (NIST, Gaithersburg, MD), Joseph T. Hodges (NIST, Gaithersburg, MD), Qiancheng Ma (NASA, Goddard Institute for Space Studies), and Andrei Vigin (Obukhov Institute of Atmospheric Physics, Moscow) in the preparation of the manuscript. Dennis Tokaryk (Mount Allison University, Sackville, NB) is acknowledged for lending the spectrum analyzer. One of the authors (J.C.) would like to thank the Government of Ontario for financial support through its program of Graduate Scholarships. This research was supported by the COMDEV/BOMEM/AES/CSA/NSERC/University of Toronto Industrial Research Chair in Remote Sounding From Space.

- ¹W. M. Elsasser, Phys. Rev. **53**, 768 (1938).
- ²A. Adel, Astrophys. J. **89**, 1 (1939).
- ³R. Anthony, Phys. Rev. **85**, 674 (1952).
- ⁴W. T. Roach and R. M. Goody, Q. J. R. Meteorol. Soc. **84**, 319 (1958).
- ⁵K. Bignell, F. Saiedy, and P. A. Sheppard, J. Opt. Soc. Am. **53**, 466 (1963).
- ⁶S. S. Penner and P. Varanasi, J. Quant. Spectrosc. Radiat. Transf. **7**, 687 (1967).
- ⁷P. Varanasi, S. Chou, and S. S. Penner, J. Quant. Spectrosc. Radiat. Transf. **8**, 1537 (1968).
- ⁸D. E. Burch and D. A. Gryvnak, in *Atmospheric Water Vapor*, edited by A. Deepak, T. D. Wilkerson, and L. H. Ruhnke (Academic, New York, 1980).
- ⁹D. E. Burch and R. L. Alt, AFGL Report No. AFGL-TR-84-0128 (Hanscom AFB, Bedford, MA, 1984).
- ¹⁰S. A. Clough, F. X. Kneizys, and R. W. Davies, Atmos. Res. **23**, 229 (1989).
- ¹¹P. Varanasi and S. Chudamani, J. Quant. Spectrosc. Radiat. Transf. **38**, 407 (1987).
- ¹²G. L. Loper, M. A. O'Neill, and J. A. Gelbwachs, Appl. Opt. **22**, 3701 (1983).
- ¹³J. S. Ryan, M. H. Hubert, and R. A. Crane, Appl. Opt. **22**, 711 (1983).
- ¹⁴J. Hinderling, M. W. Sigrist, and F. K. Kneubühl, Infrared Phys. **27**, 63 (1987).
- ¹⁵W. B. Grant, Appl. Opt. **29**, 451 (1990).
- ¹⁶R. E. Roberts, J. E. A. Selby, and L. M. Biberman, Appl. Opt. **15**, 2085 (1976).
- ¹⁷R. H. Tipping and Q. Ma, Atmos. Res. **36**, 69 (1995).
- ¹⁸Q. Ma and R. H. Tipping, J. Chem. Phys. **111**, 5909 (1999).
- ¹⁹A. O'Keefe and D. A. G. Deacon, Rev. Sci. Instrum. **59**, 2544 (1988).
- ²⁰D. Romanini and K. K. Lehmann, J. Chem. Phys. **99**, 6287 (1993).
- ²¹P. Zalicki and R. N. Zare, J. Chem. Phys. **102**, 2708 (1995).
- ²²R. T. Jongma, M. G. H. Boogaarts, I. Holleman, and G. Meijer, Rev. Sci. Instrum. **66**, 2821 (1995).
- ²³J. T. Hodges, J. P. Looney, and R. D. van Zee, Appl. Opt. **35**, 4112 (1996).
- ²⁴K. K. Lehmann and D. Romanini, J. Chem. Phys. **105**, 10263 (1996).
- ²⁵J. P. Looney, J. T. Hodges, and R. D. van Zee, in *Cavity-Ringdown Spectroscopy: An Ultratrace-Absorption Measurement Technique*, edited by K. W. Busch and M. A. Busch (American Chemical Society, MD, 1999).
- ²⁶R. D. van Zee, J. T. Hodges, and J. P. Looney, Appl. Opt. **38**, 3951 (1999).
- ²⁷A. Wexler, J. Res. Natl. Bur. Stand., Sect. A **80A**, 775 (1976).
- ²⁸A. Wexler, J. Res. Natl. Bur. Stand., Sect. A **81A**, 5 (1977).
- ²⁹V. N. Aref'ev, Izv. Akad. Nauk SSSR Ser. Fiz. **27**, 1187 (1991) [Izv. Akad. Nauk SSSR, Ser. Fiz. **27**, 863 (1991)].
- ³⁰J. C. Peterson *et al.*, Appl. Opt. **18**, 834 (1979).
- ³¹R. J. Nordstrom *et al.*, Appl. Opt. **17**, 2724 (1978).
- ³²V. N. Arefev and V. I. Dianov-Klovok, Opt. Spectrosc. **42**, 488 (1977).
- ³³J. H. McCoy, D. B. Rensch, and R. K. Long, Appl. Opt. **8**, 1471 (1969).
- ³⁴P. W. Rosenkranz, J. Chem. Phys. **83**, 6139 (1985).
- ³⁵P. W. Rosenkranz, J. Chem. Phys. **87**, 163 (1987).